AJNR

Optimal visualization of the cerebrospinal fluid on MRI.

D A Ortendahl, J P Posin, N M Hylton and C M Mills

AJNR Am J Neuroradiol 1986, 7 (3) 403-407
http://www.ajnr.org/content/7/3/403.citation

Optimal Visualization of the Cerebrospinal Fluid on MRI

Douglas A. Ortendahl,[1] Jonathan P. Posin,[1] Nola M. Hylton,[1] and Catherine M. Mills[1, 2]

The accurate delineation of cerebrospinal fluid (CSF)-filled spaces in the central nervous system (CNS) is essential for the diagnosis of many disease states, including extraaxial mass lesions, intraventricular tumors, and lesions of the spinal cord and canal. Oftentimes, the point of interest is the boundary between the CSF and the normal brain. Other times, it is important to distinguish the CSF from cortical bone. We describe here the possible strategies for visualizing the CSF and distinguishing it from other CNS structures.

This is a well-defined problem, since the parameters T1, T2, and proton density, N(H), are very different for brain, bone, and CSF. The CSF has a significantly longer T1 and T2 than does the normal brain; thus, the simplest way to distinguish these two is to use a short repetition time (TR) imaging protocol, which produces an image with brain of medium intensity and a CSF of low intensity. This was one of the earliest techniques developed [1], and two problems are associated with it. First, several investigators have shown that short TR protocols are not particularly sensitive to many of the typical disease states of the central nervous system [2]. Moreover, the delineation of gray and white matter is poor except within a relatively small range of short TR values [3]. In this range, gray matter has less intensity than white matter. Second, the dark CSF is difficult to distinguish from areas of low signal because of bone, air, or rapidly flowing blood in vessels.

It is desirable to overcome the shortcomings of short TR imaging. To do so, we can study analytically the dependence of image contrast on the acquisition parameters TE (echo time) and TR [3]. Using the tools of this technique along with the T1, T2, and N(H) values for CSF and normal white matter, which are representative of the values seen in our normal

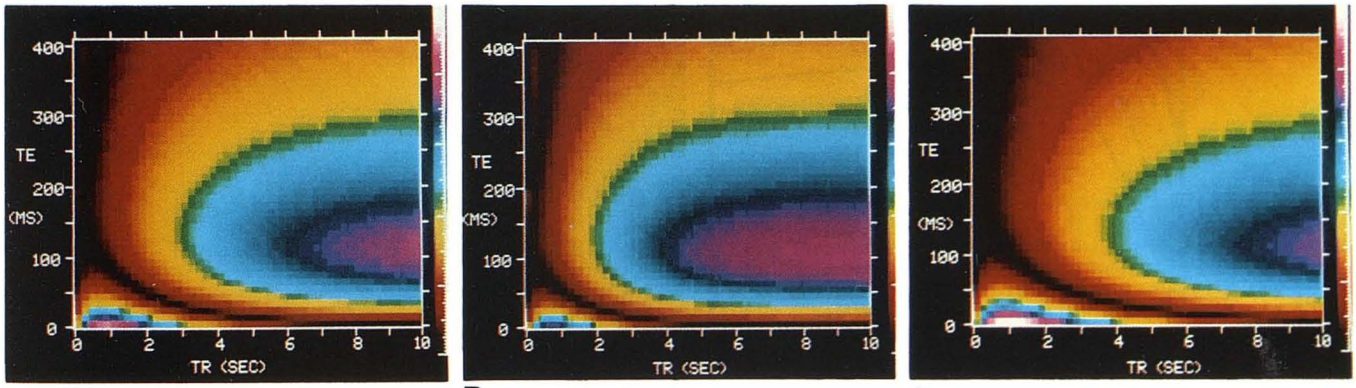

Fig. 1.—Difference maps for white matter and CSF. As a function of TE and TR, the absolute signal difference between white matter and CSF is plotted for an acquisition at that particular TE and TR. The parameters for white matter are T1 = 443 ms, T2 = 59 ms, and N(H) = 3565. In **A**, the parameters for CSF are T1 = 2679 ms, T2 = 231 ms, and N(H) = 3721. Increasing signal difference between these two tissues is shown as color changes from red or black (small or absent difference) to violet or white (large difference). In **B** and **C**, the sensitivity of the difference maps to changes in parameters is shown by varying the T1 value for CSF while using the white matter values of **A**. In **B**, the parameters for CSF are T1 = 1784 ms, T2 = 231 ms, and N(H) = 3721; in **C**, the parameters for CSF are T1 = 3571 ms, T2 = 231 ms, and N(H) = 3721.

Received May 7, 1985; accepted after revision September 4, 1985.
Presented in part at the annual meeting of the American Society of Neuroradiology, New Orleans, February 1985.
This work was supported in part by USPHS Research Career Development Award GM00493 from the NIGMS (DHHS); by USPHS Grant CA 32850 from the NCI; and by Diasonics (MRI), Inc.

[1] Radiologic Imaging Laboratory, University of California, San Francisco, 400 Grandview Drive, South San Francisco, CA 94080. Address reprint requests to D. A. Ortendahl.
[2] Present address: Diagnostic Networks, Inc., 1361 Bush Street, San Francisco, CA 94109.

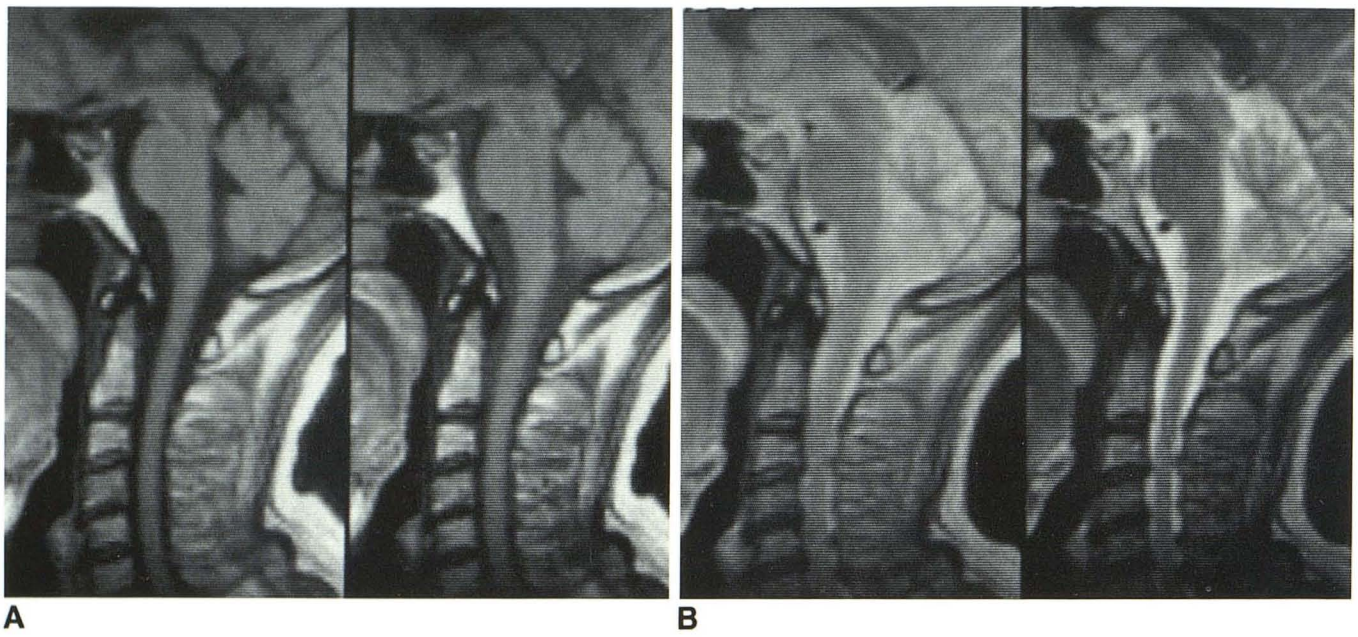

Fig. 2.—A patient with cervical radiculopathy was studied with a short (0.5 sec) (**A**) and a long (5.0 sec) (**B**) TR sequence. Although the anatomic detail is superb in the first sequence, the multiple extradural defects that compromise the cervical subarachnoid space are not delineated. First panel of each figure, TE = 28; second panel of each figure, TE = 56.

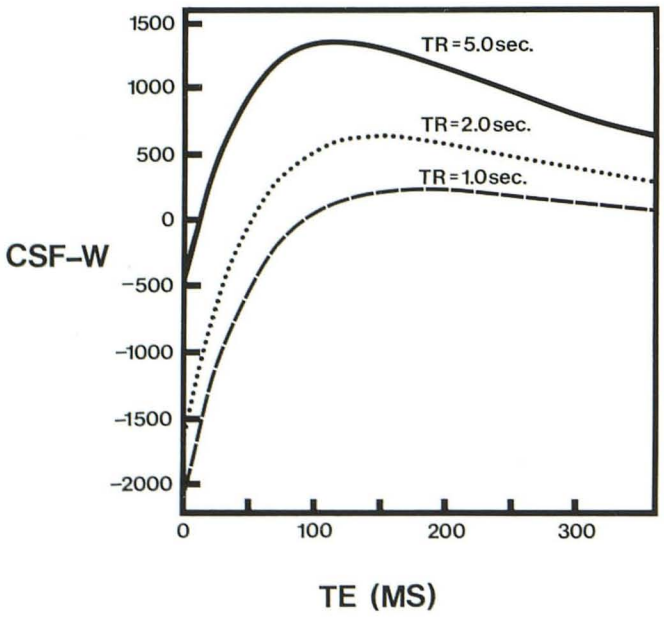

Fig. 3.—Profiles along the TE axis of the intensity difference between CSF and white matter, I(CSF) − I(W), for TR = 1.0, 2.0, and 5.0 sec. At short TR values the white matter is more intense and the intensity difference is negative.

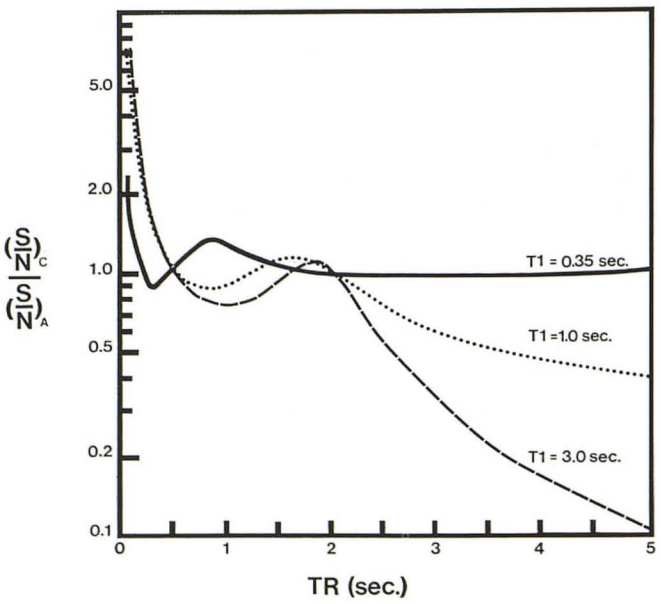

Fig. 4.—The signal-to-noise ratio of the calculated images compared with the acquired images is plotted as a function of the TR at which the calculation/acquisition is performed for four different values of T1. The original data set for the calculations is a set of TR = 0.5 sec and TR = 2.0 sec images. An equal number of data acquisitions for all images is assumed.

patient population, we plot signal difference as a function of TE and TR in Figure 1A. Two regions of high signal difference are seen. The first region at short TR and TE, where CSF is dark relative to brain, has already been discussed. The other region is at long TR. In this region CSF will have a higher signal intensity than white matter, as seen in the TR = 5.0 sec image of Figure 2. Again, bone and rapidly flowing blood are of low intensity, allowing the clear delineation of their boundaries with the CSF. In addition, sensitivity to disease in the brain is high at long TR [2]. Gray versus white matter differentiation is preserved, as discussed extensively in Ortendahl et al. [3].

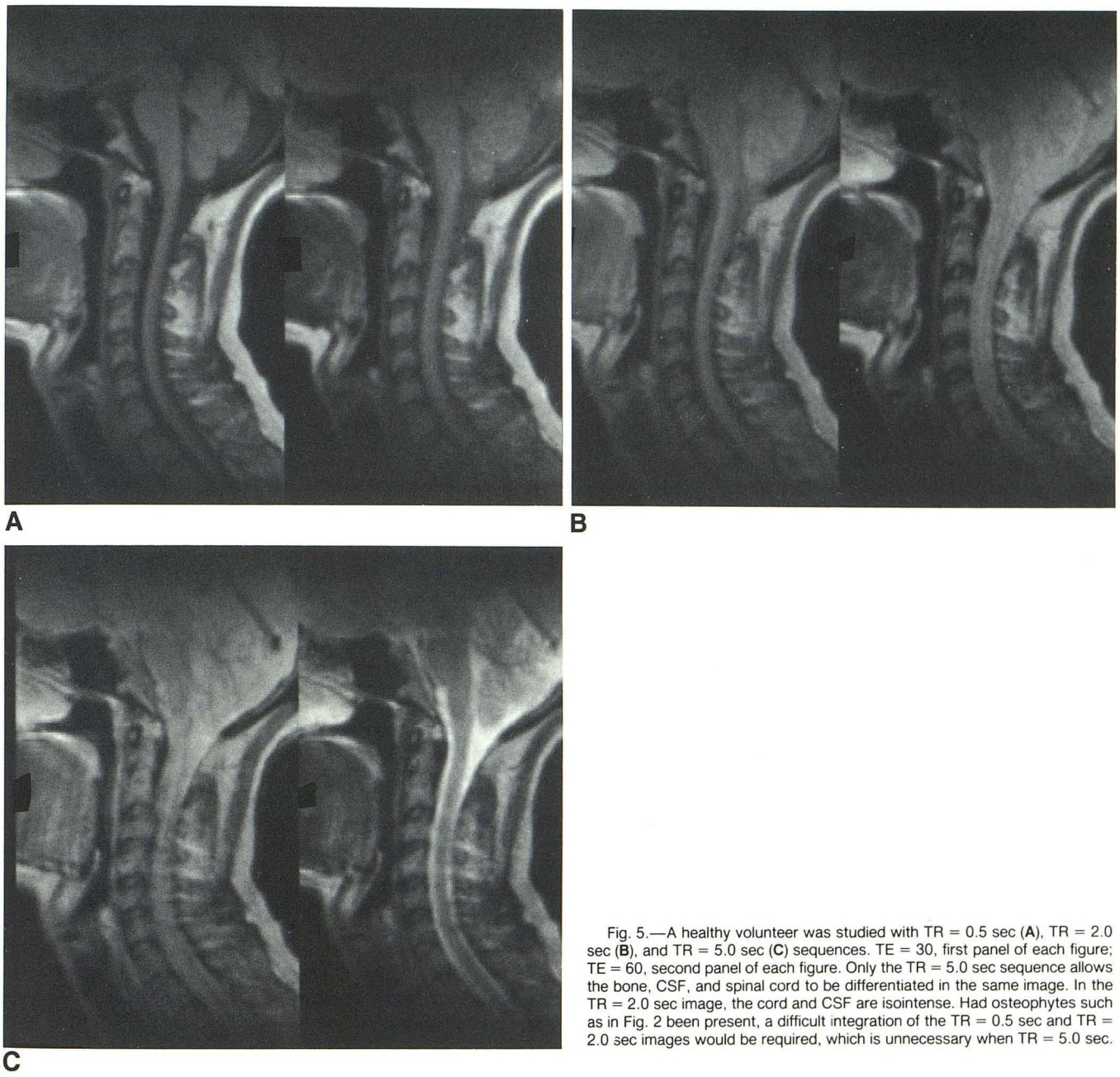

Fig. 5.—A healthy volunteer was studied with TR = 0.5 sec (**A**), TR = 2.0 sec (**B**), and TR = 5.0 sec (**C**) sequences. TE = 30, first panel of each figure; TE = 60, second panel of each figure. Only the TR = 5.0 sec sequence allows the bone, CSF, and spinal cord to be differentiated in the same image. In the TR = 2.0 sec image, the cord and CSF are isointense. Had osteophytes such as in Fig. 2 been present, a difficult integration of the TR = 0.5 sec and TR = 2.0 sec images would be required, which is unnecessary when TR = 5.0 sec.

The dark valley in Figure 1 that separates the two regions represents the area where CSF and white matter are of equal intensity, and there is a contrast reversal as the acquisition point moves across the valley from one region to another. The difference map shows that imaging with the CSF more intense than the brain and with TR<2.0 sec requires a long TE value. Even so, signal difference will not be as high as with the long TR. The image will also suffer in signal-to-noise, since signal intensity will be less with shorter TR and longer TE. In particular, the intensity of the white matter will decrease quite rapidly with increasing TE. Ultimately, as in the case of the short TR, TE region, distinguishing white matter from other low-intensity structures will be difficult. In this long TE region, as we increase TE we are moving tangent to the isodifference line, giving poor sensitivity to changes in T2. There is little return in terms of signal difference from increasing TE when compared with the loss of signal within the brain. On the other hand, the gradient with respect to TR is steep, increasing the sensitivity to small changes in T1. The technique is not as robust, and the results will be less predictable.

Consider now the long TR region. The large area of approximately equal signal difference indicates that it is a forgiving technique, not overly sensitive to changes in TR or, equivalently, in T1. In this region, contrast is determined primarily by T2 and N(H). Although the maximum in the plot is at TR = 10.0 sec, it is possible to shorten TR to 5.0 sec

with only a 20% reduction in signal difference. In Figure 3 we show profiles of the signal difference as a function of TE for three different values of TR. The advantage of the long TR is quite apparent. The peak in the curve at TR = 5.0 sec also shows clearly that there is no advantage in using a TE value longer than this peak point.

To test the sensitivity of these conclusions to the specific tissue parameters used to make the difference map, in Figures 1B and 1C we show two additional difference maps where the T1 values for CSF are one-third less or one-third more than those used in Figure 1A. The maps are different, but the basic conclusion concerning strategy for imaging CSF remains the same. Short TR, long TE protocols are not as effective as the longer TR acquisitions. As would be expected, the "forgiving" long TR region moves to shorter TR values when the T1 of the CSF is shortened and to longer TR points when the T1 is lengthened.

Since TR = 5.0 sec acquisitions require increased imaging time, it is appropriate to ask whether it is possible to use two shorter TR protocols and use the calculated T1, T2, and N(H) images to compute the long TR image [3]. A major concern in such a computation would be propagated noise [4]. In Figure 4 we investigate the quality of images calculated at various TRs by plotting the ratio of the signal-to-noise ratio of the calculated image and the acquired image as a function of the desired TR. It is assumed that the original data set was acquired at TR = 0.5 sec and TR = 2.0 sec, which we have previously shown to offer good signal-to-noise levels in computed T1 images [3]. The comparison is done for an equal number of acquisitions of the data in all images. For short TRs the signal-to-noise ratio is better for the calculated images mainly because the signal intensity is low and the extrapolation from an accurate data set can produce a better estimate than the real acquisition, which has the same noise level as at other TR values. As required, the calculated image is equivalent to the acquired image at 0.5 and 2.0 sec. In between these two data points, the calculated image benefits from interpolation, especially near 2.0 sec. Unfortunately, in the interesting diagnostic region of long TR, the calculated images do poorly. For short T1 values the calculations are almost as good as the acquired image, since the 2.0-sec data point is so close to the asymptotic value. For the longer T1 values, which are of interest for this problem, the signal-to-noise ratio of the calculated images deteriorates with respect to the acquired image. This indicates that calculated long TR images for visualizing CSF may not be of sufficiently good quality to be useful diagnostically.

An alternative strategy would be to use two separate acquisitions, such as TR = 0.5 sec and TR = 2.0 sec. This is illustrated in Figure 5, where the low-intensity CSF is separated from the higher-intensity spinal cord in the TR = 0.5 sec image and the CSF is separated from the low-intensity bone with the TR = 2.0 sec acquisition. The problem with using only the TR = 2.0 sec image is apparent, since the CSF and spinal cord are isointense while with the TR = 5.0 sec image, the bone, CSF, and spinal cord are well differentiated. The use of multiple images requires that the physician integrate the information contained in these different images. For imaging the spinal cord, the precise relationship between any protruding osteophytes and the spinal cord is extremely important, and discerning these small distances from multiple images can be difficult. This task would be much easier in the TR = 5.0 sec image, where the relationships are contained in a single image.

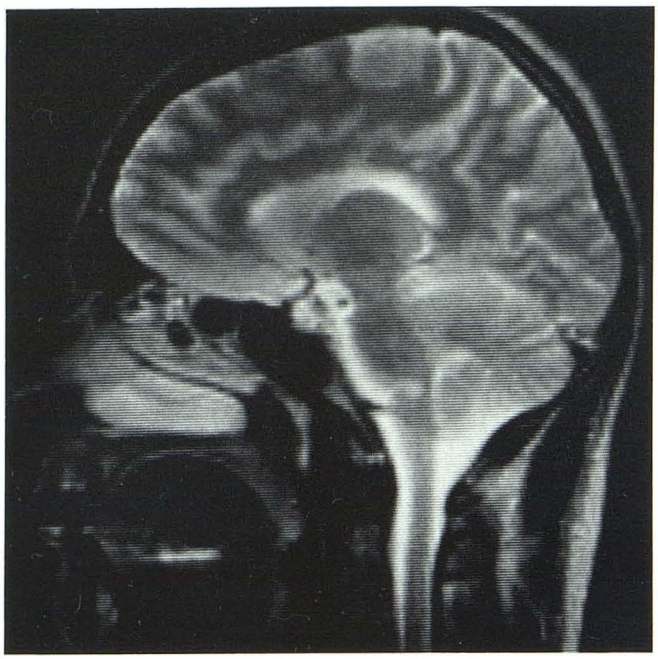

Fig. 6.—A patient with multiple sclerosis is imaged with TR = 5.0 sec and TE = 56 ms. The periventricular plaque shows excellent tissue discrimination while, simultaneously, CSF spaces show high intensity, allowing discrimination from such lower signal structures as bone.

The long TR protocols are efficient. The use of relatively short TE values (<70 ms) expedites the use of multisection techniques by allowing the accumulation of additional sections rather than spending the time waiting for late echoes. The excellent signal-to-noise ratio allows the use of as few as two acquisitions of the data, making it possible to obtain a 20-section sagittal neck study in 21 min. While not all these sections are needed, the region of interest can be fully covered in an imaging time consistent with current MRI (magnetic resonance imaging) practice. Sensitivity to disease in the brain is excellent, as demonstrated by the multiple sclerosis case in Figure 6. On the other hand, this is not a completely universal screening sequence. The loss of contrast between CSF and areas of pathology, which can sometimes occur at long TE values as relative CSF intensity increases, can also occur at long TR values. This would obscure, for instance, periventricular edema and confluent periventricular multiple sclerosis plaques. For such cases the solution is not a short TR image but one at an intermediate value, such as 1.5 or 2.0 sec, where lesions are typically more intense than brain parenchyma, and at TE = 28 ms, where lesions and brain parenchyma are both more intense than CSF. Such sequences have been shown to be extremely effective in demonstrating diseases such as multiple sclerosis [2, 5].

In conclusion, the use of long TR protocols for visualizing CSF spaces in the CNS is an effective method of discriminating CSF from other structures and at the same time for giving good sensitivity to disease in the neural tissue not immediately adjacent to CSF spaces. At present, the major application of this technique appears to be in evaluating disease of the spinal cord and canal.

REFERENCES

1. Norman D, Brant-Zawadski M, Mills CM. Magnetic resonance imaging of the spinal cord. In: Moss AA, Ring EJ, Higgins CB, eds. *NMR, CT, and interventional radiology*. San Francisco: Radiology Research and Education Foundation, **1984**:275–279
2. Brant-Zawadski M, Norman D, Newton TH, et al. Magnetic resonance of the brain the optimal screening technique. *Radiology* **1984**;152:71–77
3. Ortendahl DA, Hylton NM, Kaufman L, Watts J, Crooks LE, Mills CM, Stark D. Analytical tools for MRI. *Radiology* **1984**;153:479–488
4. Ortendahl DA, Hylton NM, Kaufman L, Crooks LE. Signal to noise in derived NMR images. *Magnetic Resonance Med* **1984**;1:316–338
5. Lukes SA, Crooks LE, Aminoff MJ, et al. Nuclear magnetic resonance imaging in multiple sclerosis. *Ann Neurol* **1983**; 13:592–601